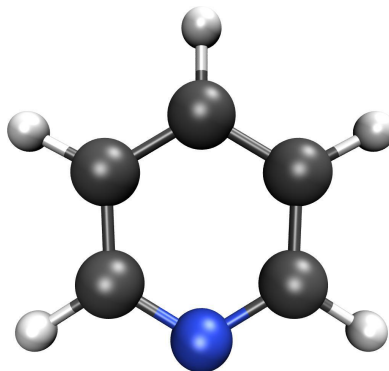




A Report On The Calculation Of The Optimised Structure, Vibrational Frequencies And Excited States Of Pyridine At The PBE1PBE/6-31G(d,p) Level

osl - 16th June 2022



Abstract

The calculation of optimised structure, vibrational frequencies and excited states for the system 'Pyridine' is presented, accompanied by automated analysis and image generation provided by the Silico software package. The calculations were performed using the Gaussian software package(s) at the PBE1PBE/6-31G(d,p) level of theory. The total self-consistent field (SCF) energy of the system was found to be -6748.61 eV after 5 steps. The highest-occupied molecular orbital (HOMO) and lowest-unoccupied molecular orbital (LUMO) were calculated to be -7.28 and -0.51 eV respectively, corresponding to a HOMO-LUMO band gap of 6.77 eV. The permanent dipole moment (PDM) was calculated to be 2.51 D. The most intense vibrational frequencies were calculated to be at 724, 1028, 1493, 1667 and 3203 cm⁻¹, and there were zero negative frequencies. In total, 20 excited states were calculated with singlet and triplet multiplicity. The most intense absorption peaks were calculated to be at 154, 180, 213 and 243 nm. The lowest energy singlet and triplet excited states (S_1 and T_1) were calculated to be 5.07 and 4.28 eV (244 and 290 nm) respectively, corresponding to a singlet/triplet splitting energy (ΔE_{ST}) of 0.80 eV.

Table 1: Summary of overall calculation metadata. [a]: The date and time at which the calculation was completed. [b]: Total combined duration in real-time (wall-time) for all components of the calculation. [c]: Temperature used for thermochemistry analysis. [d]: Pressure used for thermochemistry analysis.

Calculation no.	Date ^[a]	Duration ^[b]	Success (Converged)	Computational package	Level of theory	Calculations	Wavefunction	Multiplicity	T ^[c] / K	P ^[d] / atm
Combined	16/06/2022 00:14:35	15 m, 20 s	True (True)	Gaussian (2016+C.01)	PBE1PBE/6-31G(d,p)	Optimisation, Frequencies, Excited States	restricted	1 (singlet)	N/A	N/A
1	15/06/2022 23:24:49	1 m, 23 s	True (True)	Gaussian (2016+C.01)	PBE1PBE/6-31G(d,p)	Optimisation, Frequencies	restricted	1 (singlet)	298.15	1.0
2	15/06/2022 23:33:59	4 m, 13 s	True (N/A)	Gaussian (2016+C.01)	PBE1PBE/6-31G(d,p)	Excited States	restricted	1 (singlet)	N/A	N/A
3	16/06/2022 00:14:35	9 m, 42 s	True (True)	Gaussian (2016+C.01)	PBE1PBE/6-31G(d,p)	Optimisation, Excited States	restricted	1 (singlet)	N/A	N/A

Summary Of Results

Scf Energy

Table 2: Summary of SCF energy properties.

No. of steps	5
Final energy	-6748.6129 eV
Final energy	-651,142 kJ·mol ⁻¹

Geometry

Table 3: Summary of geometry properties.

Formula	C ₅ NH ₅
Exact mass	79.0422 g·mol ⁻¹
Molar mass	79.0999 g·mol ⁻¹
Alignment method	Minimal
X extension	4.31 Å
Y extension	3.89 Å
Z extension	0.00 Å
Linearity ratio	0.10
Planarity ratio	1.00

Molecular Orbitals

Table 4: Summary of HOMO & LUMO properties.

E _{HOMO,LUMO}	6.77 eV
E _{HOMO}	-7.28 eV

E_{LUMO} -0.51 eV

Permanent Dipole Moment

Table 5: Summary of the permanent dipole moment properties.

Total	2.51 D
X axis angle	90.00 °
XY plane angle	0.00 °

S₁ Transition Dipole Moment

Table 6: Summary of the transition (S₁) dipole moment (TDM) properties μ : Electric TDM. m: Magnetic TDM. $\theta_{\mu,x}$ and $\theta_{m,x}$: Angle between μ or m and the x-axis. $\theta_{\mu,xy}$ and $\theta_{m,xy}$: Angle between μ or m and the xy-plane. $\theta_{\mu,m}$: Angle between the electric and magnetic TDM. g_{lum}: Dissymmetry factor.

μ	0.59 D
$\theta_{\mu,x}$	90.00 °
$\theta_{\mu,xy}$	89.98 °
$m^{[d]}$	0.69 a.u.
$\theta_{m,x}$	0.00 °
$\theta_{m,xy}$	0.00 °
μ (Gaussian-CGS)	5.88e-19 esu·cm
m (Gaussian-CGS)	6.41e-21 erg·G ⁻¹
	90.00 °

$\theta_{\mu,m}$	
$\cos(\theta_{\mu,m})$	0.00
g_{lum}	0.000

Vibrations

Table 7: Summary of the properties of the calculated vibration frequencies.

No. frequencies	27
Simulated peaks	724, 1028, 1493, 1667 and 3203 ... cm ⁻¹
No. negative frequencies	0
Negative frequencies	N/A

Excited States

Table 8: Summary of the calculated excited states. E_x : The energy of excited state x . λ_x : The wavelength of a photon of equivalent energy to excited state x . f_x : The oscillator strength of the excited state transition x . ΔE_{xy} : The difference in energy between the lowest excited states of multiplicity x and y .

No. calculated singlets	10
E_{S_1}	5.07 eV
λ_{S_1} (colour, CIE)	244 nm (Ultraviolet ■, (0.00, 0.00))
f_{S_1}	0.01
No. calculated triplets	10
E_{T_1}	4.28 eV
λ_{T_1} (colour, CIE)	290 nm (Ultraviolet ■, (0.00, 0.00))
f_{T_1}	0.00
ΔE_{ST}	0.80 eV
Simulated Absorption Peaks	154, 180, 213 and 243 nm

Adiabatic S₁ Emission

Table 9: Summary of the adiabatic emission from the S_1 state.

Excited energy	-6743.99 eV
Excited multiplicity	Singlet
Ground energy	-6748.61 eV
Ground multiplicity	Singlet
Emission type	Fluorescence
S_1 energy	4.62 eV
S_1 wavelength (colour, CIE)	268 nm (Ultraviolet ■, (0.00, 0.00))
S_1 oscillator strength	0.00
S_1 rate	5.01e+07 /s ⁻¹

Vertical S₁ Emission

Table 10: Summary of the vertical emission from the S_1 state.

Excited energy	-6743.99 eV
Excited multiplicity	Singlet
Ground energy	-6748.11 eV
Ground multiplicity	Singlet
Emission type	Fluorescence

S_1 energy	4.12 eV
S_1 wavelength (colour, CIE)	301 nm (Ultraviolet ■, (0.00, 0.00))
S_1 oscillator strength	0.00
S_1 rate	3.54e+07 /s ⁻¹

Methodology

Metadata

This report was generated from the combined results of three individual calculations. The individual metadatas for each separate calculation are presented in the following sections, and the overall calculation was performed using the **Gaussian (2016+C.01)** program, the **DFT** method with the **PBE1PBE** functional and the **6-31G(d,p)** basis set. It was completed on the **16th June 2022** after a total duration of **15 m, 20 s** and **finished successfully**. The base multiplicity of the system under study was **1 (singlet)**. Finally, a **restricted wavefunction** was used, resulting in a single set of doubly occupied orbitals. The full calculation metadata is tabulated in table 1.

The calculation of the optimised structure and vibrational frequencies was performed using the **Gaussian (2016+C.01)** program, the **DFT** method with the **PBE1PBE** functional and the **6-31G(d,p)** basis set. It was completed on the **15th June 2022** after a total duration of **1 m, 23 s** and **finished successfully**. The base multiplicity of the system under study was **1 (singlet)**. Finally, a **restricted wavefunction** was used, resulting in a single set of doubly occupied orbitals.

The calculation of the excited states was performed using the **Gaussian (2016+C.01)** program, the **DFT** method with the **PBE1PBE** functional and the **6-31G(d,p)** basis set. It was completed on the **15th June 2022** after a total duration of **4 m, 13 s** and **finished successfully**. The base multiplicity of the system under study was **1 (singlet)**. Finally, a **restricted wavefunction** was used, resulting in a single set of doubly occupied orbitals.

The calculation of the optimised structure and excited states was performed using the **Gaussian (2016+C.01)** program, the **DFT** method with the **PBE1PBE** functional and the **6-31G(d,p)** basis set. It was completed on the **16th June 2022** after a total duration of **9 m, 42 s** and **finished successfully**. The base multiplicity of the system under study was **1 (singlet)**. Finally, a **restricted wavefunction** was used, resulting in a single set of doubly occupied orbitals.

Analysis

The report presented here was generated using the Silico software package. This toolset relies upon a number of third-party applications and libraries which should be cited appropriately in derivative works. In particular, the calculation results described within were parsed by the cclib library.¹ Scientific constants which were used, among other things, for the interconversion of scientific units were provided by SciPy.² Commission internationale de l'éclairage (CIE) coordinates, along with visual representations of the equivalent colour, were calculated using the Colour Science library.³ Emission rate constants (k_e) were calculated according to the method developed by Shizu and Kaji⁴ as described by formula 1, where ΔE_e is the energy of emission, ϵ_0 is the vacuum permittivity constant, \hbar is the reduced Planck constant (the Dirac constant), c is the speed of light and μ_e is the transition dipole moment of the emission.

$$k_e = \frac{4 \Delta E_e}{3 \epsilon_0 \hbar^4 c^3} \mu_e \quad 1$$

Three-dimensional plots of atom positions and calculated densities, including molecular orbitals, were rendered using Visual Molecular Dynamics (VMD)⁵ and the Tachyon ray-tracer.⁶ Finally, two-dimensional graphs were plotted using the Matplotlib library,⁷ while this report itself was prepared using the Mako template library⁸ and the Weasyprint library⁹, the latter of which was responsible for generation of the PDF file.

Discussion

Total SCF Energy

The total energy of the system was calculated at the **self-consistent field (SCF)** level, corresponding to the energy calculated by the density-functional theory (DFT) method, over a total of five steps, the results of which are displayed in figure 1. The energy calculated by the final step was -6748.61 eV, corresponding to -651,142 KJmol⁻¹. A plot of the total SCF electron density is shown in figure 2.

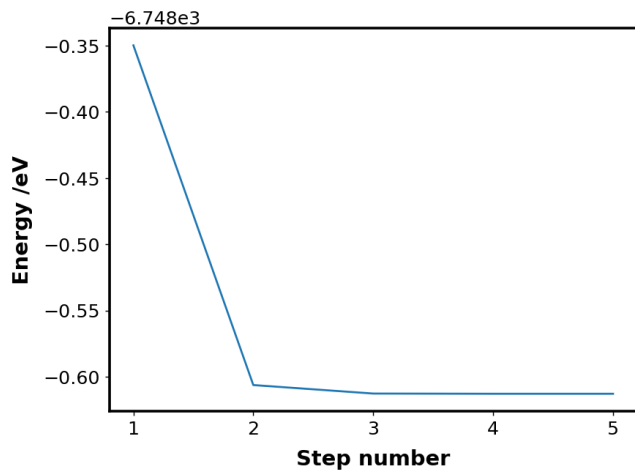


Figure 1: Graph of calculated energies at the self-consistent field (SCF) level.

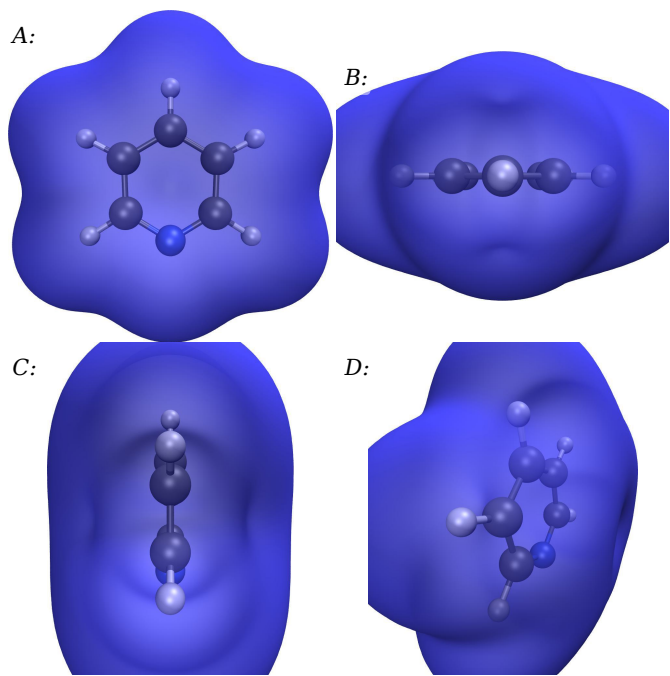


Figure 2: Plot of the total SCF electron density, plotted with an isovalue of 0.0004. A: In the X/Y plane, B: In the X/Z plane, C: In the Z/Y plane, D: 45° to the axes.

Geometry

The **empirical formula** of the studied system was C₅NH₅, corresponding to a **molecular mass** of 79.10 gmol⁻¹ and an **exact mass**, considering only specific atomic isotopes, of 79.04 gmol⁻¹. The molecular geometry was aligned to the cartesian (X, Y and Z) axes by the **Minimal (MIN)** method. Using this method, the **extent of the molecular system** in the X, Y and Z axes (L_X, L_Y and L_Z, corresponding to the molecular width, length and height respectively) was determined to be 4.31, 3.89 and 0.00 Å respectively. These extensions give rise to a **molecular linearity ratio** (1-(L_Y/L_X)) and **planarity ratio** (1-(L_X/L_Y)) of 0.10 and 1.00 respectively.

Permanent Dipole Moment

The calculated **permanent dipole moment** was 2.51 D, with a vector (x,y,z) of 0.00, 2.51, -0.00 D. The angle between the dipole moment vector and the x-axis was 90.00 °, while the angle between the dipole moment and the xy-plane was 0.00 °. A plot of the permanent dipole moment is shown in figure 3.

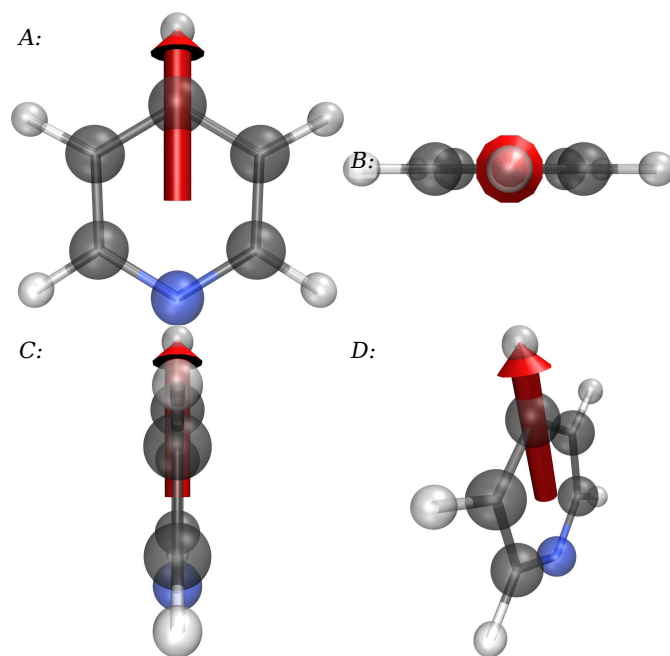


Figure 3: The permanent dipole moment (red arrow) plotted against the aligned molecular geometry with a scale of $1 \text{ \AA} = 1.0 \text{ D}$. A: In the X/Y plane, B: In the X/Z plane, C: In the Z/Y plane, D: 45° to the axes.

Transition (S_1) Dipole Moment

The calculated **electric (TEDM, μ)** and **magnetic (TMDM, m)** transition dipole moments between the ground state and the S_1 excited state were 0.59 D and 0.69 au respectively. The corresponding vector components (x,y,z) were $\mu = 0.00, -0.00, 0.59 \text{ D}$ and $m = 0.69, 0.00, 0.00 \text{ au}$. In comparison to the molecular geometry, the angle between each dipole moment and the longest axis of the molecule (the x-axis) was $\theta_{\mu,x} = 90.00^\circ$ and $\theta_{m,x} = 0.00^\circ$, while the angle between each dipole moment and the xy-plane was $\theta_{\mu,xy} = 89.98^\circ$ and $\theta_{m,xy} = 0.00^\circ$. In Gaussian-CGS units, in which the magnetic and electric transition dipole moments can be directly compared, the magnitude of each dipole moment was $\mu = 5.88e-19 \text{ esu}\cdot\text{cm}$ and $m = 6.41e-21 \text{ erg}\cdot\text{G}^{-1}$, while the **angle between the two dipole moments** was $\theta_{\mu,m} = 90.00^\circ$. Correspondingly, the cosine of the angle was $\cos(\theta_{\mu,m}) = 0.00$, and the **dissymmetry factor** of the excited state transition was $g_{\text{lum}} = 0.000$. A plot of the electric and magnetic transition dipole moments is shown in figure 4.

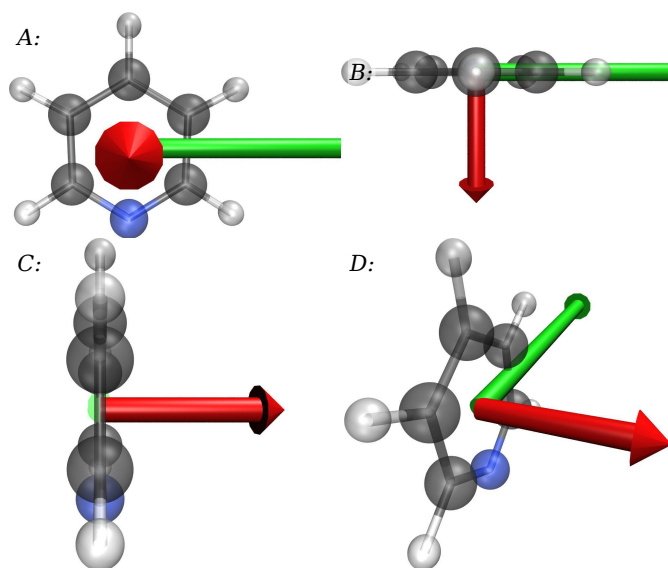


Figure 4: The electric (red arrow) and magnetic (green arrow) transition (S_1) dipole moment plotted against the aligned molecular geometry with a scale of $1 \text{ \AA} = 0.2 \text{ D} = 0.1 \text{ au}$. A: In the X/Y plane, B: In the X/Z plane, C: In the Z/Y plane, D: 45° to the axes.

Molecular Orbitals

In total, 115 doubly occupied molecular orbitals were calculated, divided into 21 occupied orbitals and 94 unoccupied (or virtual) orbitals. The calculated energies of the **HOMO** and **LUMO** were -7.28 and -0.51 eV respectively, corresponding to a **HOMO-LUMO band gap** of 6.77 eV (figure 16). Plots of the orbital density for the HOMO-5, HOMO-4, HOMO-3, HOMO-2, HOMO-1, HOMO, LUMO, LUMO+1, LUMO+2 and LUMO+4 are shown in figures 5-11 and 13-15 respectively, while the orbital overlap between the HOMO and LUMO is shown in figure 12.

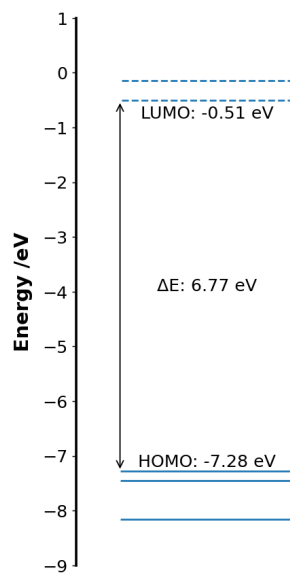


Figure 16: Graph of the calculated molecular orbital energies in close proximity to the HOMO-LUMO gap. Solid lines: occupied orbitals, dashed lines: virtual orbitals.

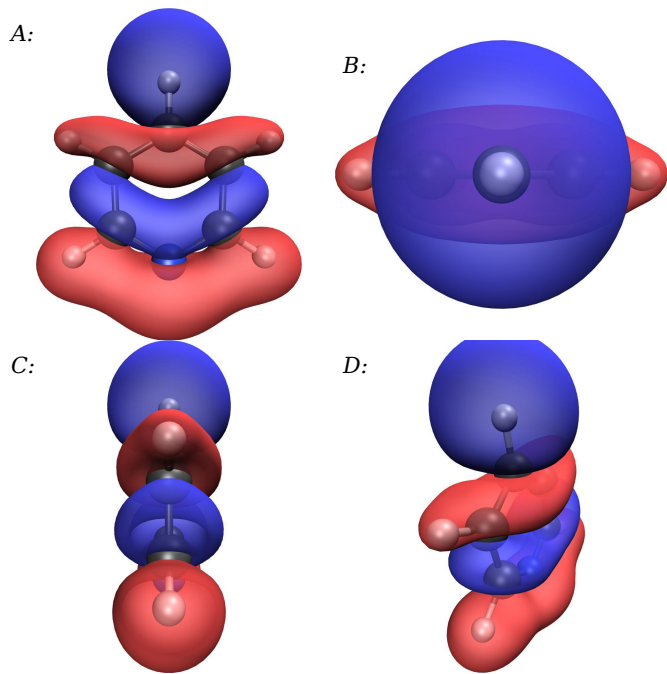


Figure 5: Orbital density plots of the HOMO-5, plotted with isovalue: 0.02. A: In the X/Y plane, B: In the X/Z plane, C: In the Z/Y plane, D: 45° to the axes.

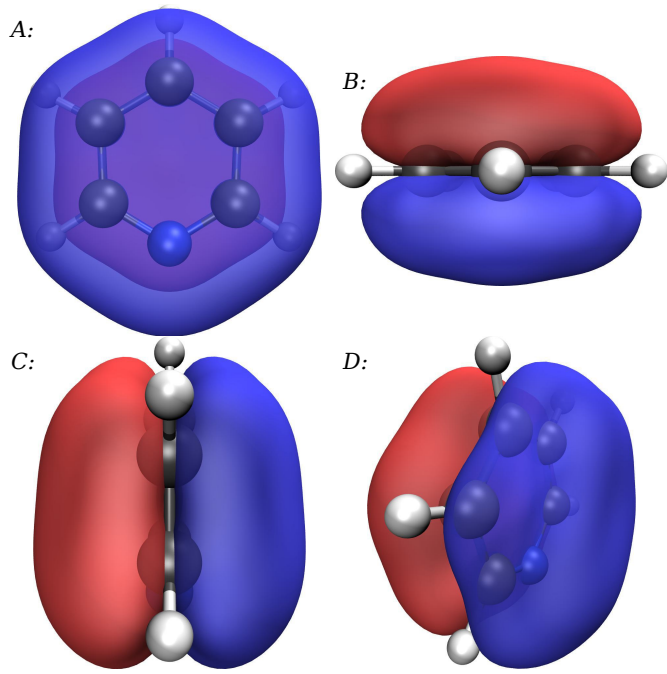


Figure 6: Orbital density plots of the HOMO-4, plotted with isovalue: 0.02. A: In the X/Y plane, B: In the X/Z plane, C: In the Z/Y plane, D: 45° to the axes.

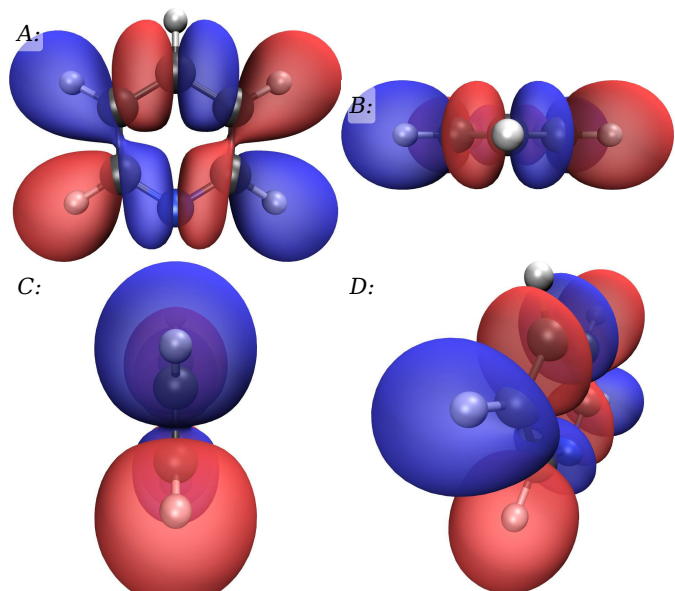


Figure 7: Orbital density plots of the HOMO-3, plotted with isovalue: 0.02. A: In the X/Y plane, B: In the X/Z plane, C: In the Z/Y plane, D: 45° to the axes.

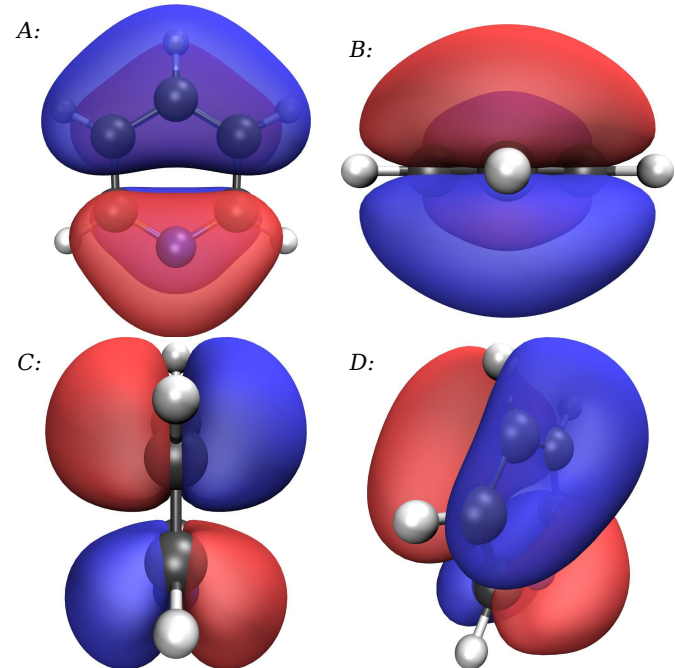


Figure 8: Orbital density plots of the HOMO-2, plotted with isovalue: 0.02. A: In the X/Y plane, B: In the X/Z plane, C: In the Z/Y plane, D: 45° to the axes.

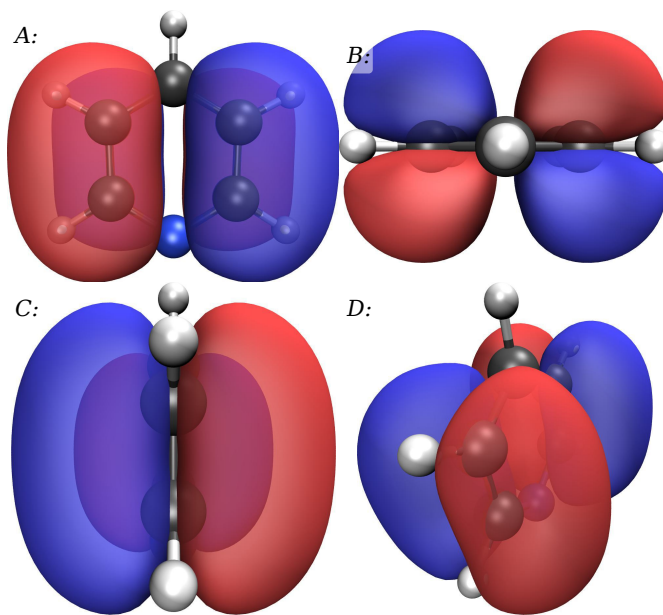


Figure 9: Orbital density plots of the HOMO-1, plotted with isovalue: 0.02. A: In the X/Y plane, B: In the X/Z plane, C: In the Z/Y plane, D: 45° to the axes.

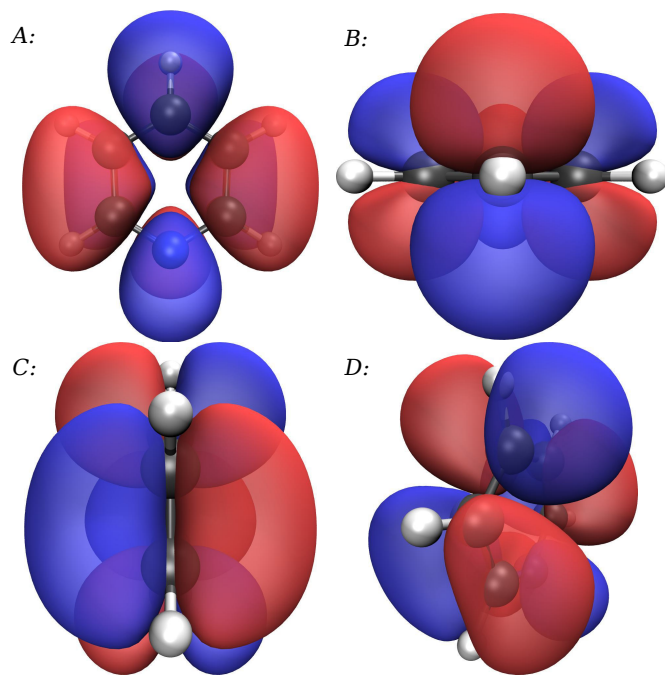


Figure 11: Orbital density plots of the LUMO, plotted with isovalue: 0.02. A: In the X/Y plane, B: In the X/Z plane, C: In the Z/Y plane, D: 45° to the axes.

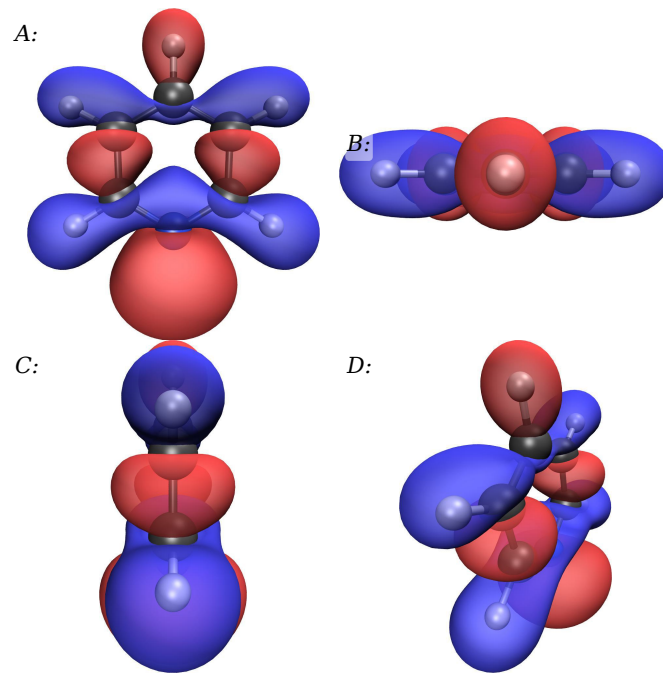


Figure 10: Orbital density plots of the HOMO, plotted with isovalue: 0.02. A: In the X/Y plane, B: In the X/Z plane, C: In the Z/Y plane, D: 45° to the axes.

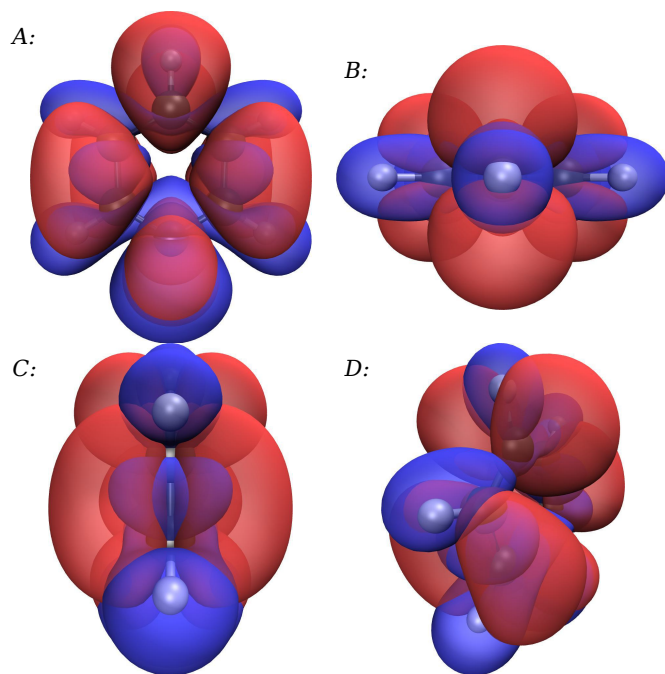


Figure 12: Orbital density plots of the HOMO (blue) and LUMO (red), plotted simultaneously with isovalue: 0.02. A: In the X/Y plane, B: In the X/Z plane, C: In the Z/Y plane, D: 45° to the axes.

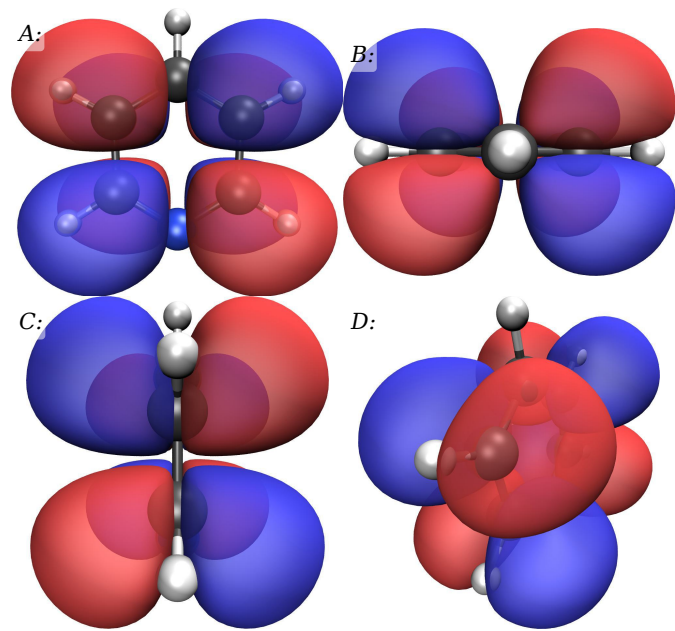


Figure 13: Orbital density plots of the LUMO+1, plotted with isovalue: 0.02. A: In the X/Y plane, B: In the X/Z plane, C: In the Z/Y plane, D: 45° to the axes.

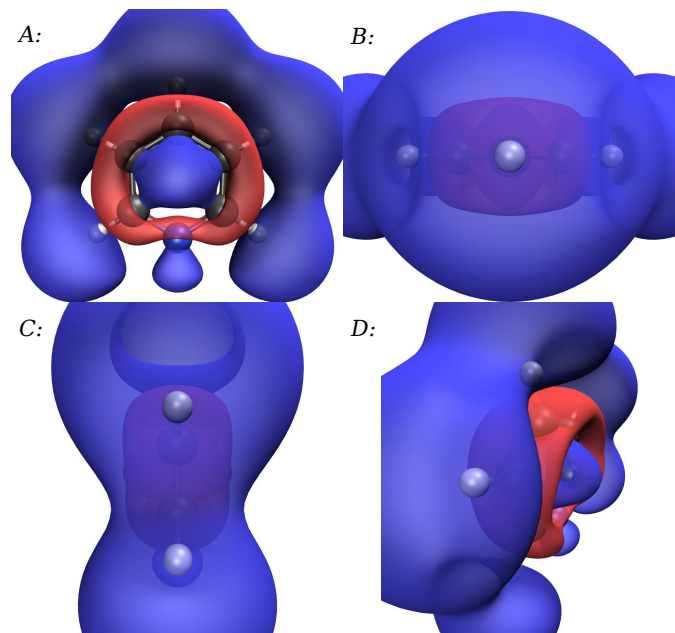


Figure 14: Orbital density plots of the LUMO+2, plotted with isovalue: 0.02. A: In the X/Y plane, B: In the X/Z plane, C: In the Z/Y plane, D: 45° to the axes.

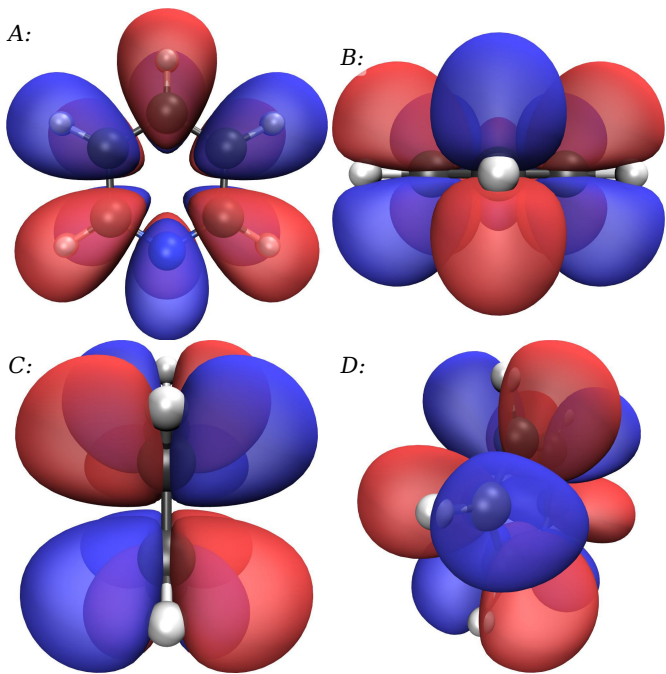


Figure 15: Orbital density plots of the LUMO+4, plotted with isovalue: 0.02. A: In the X/Y plane, B: In the X/Z plane, C: In the Z/Y plane, D: 45° to the axes.

Vibrational Frequencies

The energies of a total of 27 vibrational transitions were calculated and vibrational absorption peaks were simulated using a gaussian function with full-width at half maximum (FWHM) of 80 cm⁻¹. From this analysis the **five most intense vibrational peaks** were found at 724, 1028, 1493, 1667 and 3203 cm⁻¹. The full simulated vibrational frequency spectrum is shown in figure 17. Finally there were zero **calculated negative frequencies**.

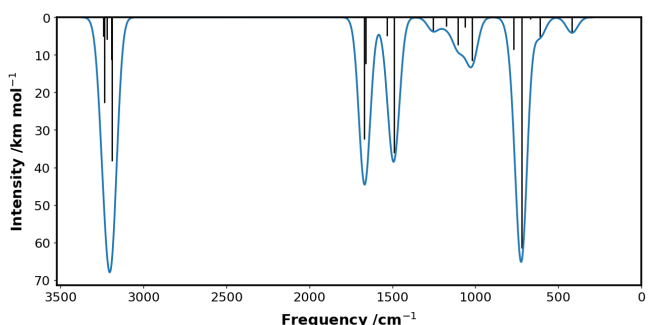


Figure 17: Graph of simulated vibrational spectrum. Calculated vibrational frequencies are shown as vertical black bars while simulated peaks with a gaussian function with FWHM: 80 cm⁻¹ are shown as a blue line. Peaks can be found at: 417, 724, 1028, 1249, 1493, 1667 and 3203 cm⁻¹.

Excited States

In total, the energies of 20 electronic excited states were calculated (figure 18), consisting of 10 states with a multiplicity of singlet and 10 of multiplicity triplet. The energy of the lowest **singlet excited state (S₁)** was 5.07 eV, corresponding to absorption by a photon with a wavelength of 244 nm, an ultraviolet 'color' ■ and CIE coordinates of (0.00, 0.00), while the energy of the T₁ was 4.28 eV (290 nm, ultraviolet ■, CIE: (0.00, 0.00)). The difference in energy between the S₁ and T₁ excited states (ΔE_{ST}) was therefore 0.80 eV. A complete table of the calculated excited state properties is available in table 11. In

addition, an electronic transition spectrum was simulated using a gaussian function with full-width at half maximum (FWHM) of 0.40 eV, from which the **four most intense peaks** were found at 154, 180, 213 and 243 nm. The full simulated absorption spectrum is shown in figure 19. Finally, **natural transition orbitals (NTOs)** were calculated for the S_1 , S_2 , S_3 , S_4 , S_5 , S_6 , S_7 , S_8 , S_9 and S_{10} excited states and are shown in figures 20-29.

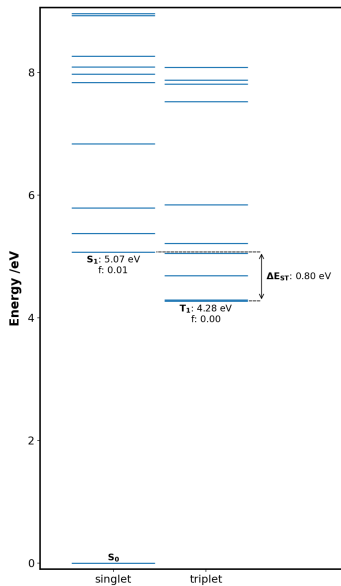


Figure 18: Graph of the calculated excited states. f : oscillator strength of the relevant ground to excited state transition.

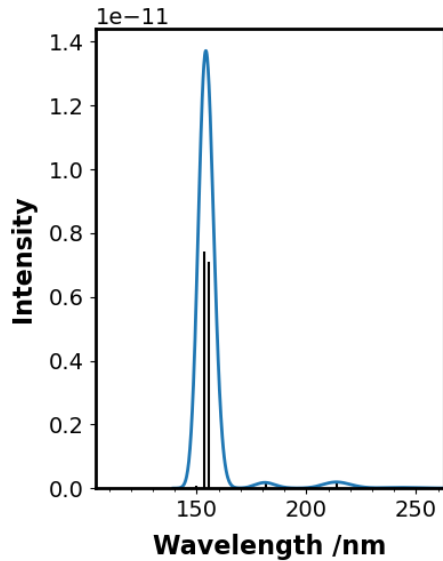


Figure 19: Graph of the simulated absorption spectrum. Excited states are shown as vertical black lines, while peaks simulated with a gaussian function with FWHM: 0.40 eV are shown as a blue line. Peaks can be found at: 154, 180, 213 and 243 nm.

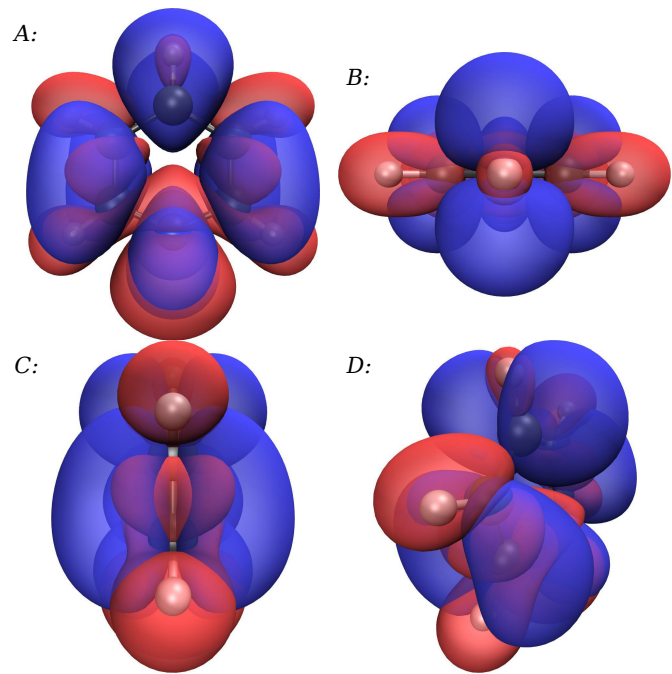


Figure 20: Density plot of the NTO hole (blue) & electron (red) of the S_1 state, plotted with isovalue: 0.02. A: In the X/Y plane, B: In the X/Z plane, C: In the Z/Y plane, D: 45° to the axes.

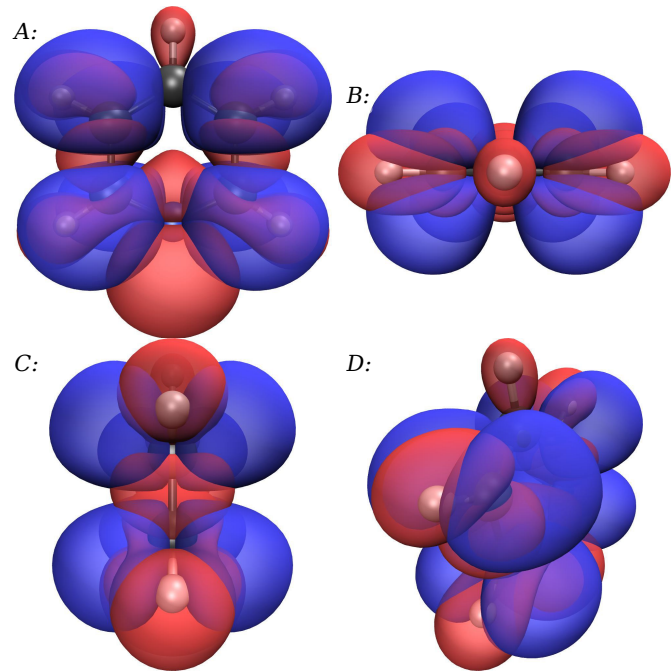


Figure 21: Density plot of the NTO hole (blue) & electron (red) of the S_2 state, plotted with isovalue: 0.02. A: In the X/Y plane, B: In the X/Z plane, C: In the Z/Y plane, D: 45° to the axes.

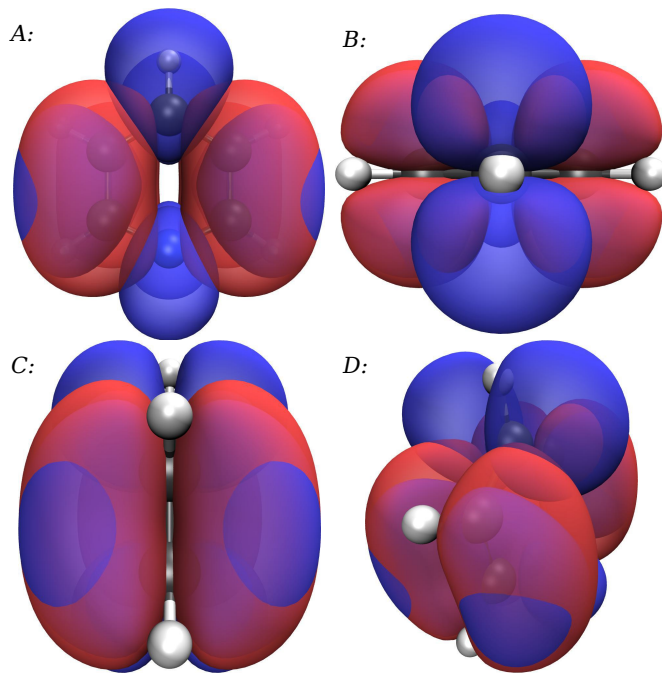


Figure 22: Density plot of the NTO hole (blue) & electron (red) of the S_3 state, plotted with isovalue: 0.02. A: In the X/Y plane, B: In the X/Z plane, C: In the Z/Y plane, D: 45° to the axes.

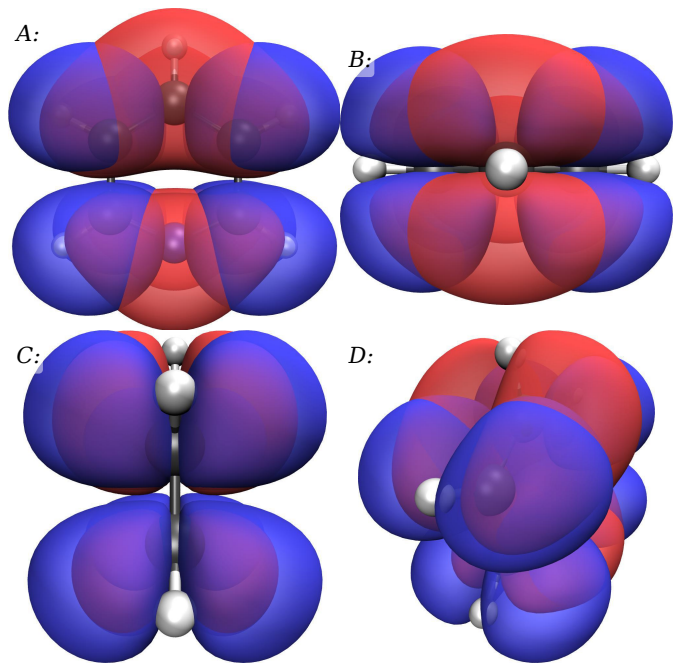


Figure 24: Density plot of the NTO hole (blue) & electron (red) of the S_5 state, plotted with isovalue: 0.02. A: In the X/Y plane, B: In the X/Z plane, C: In the Z/Y plane, D: 45° to the axes.

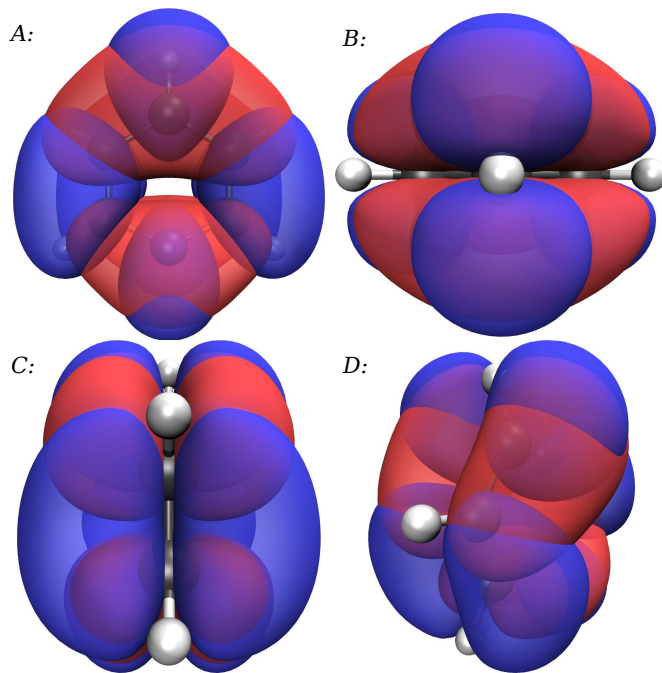


Figure 23: Density plot of the NTO hole (blue) & electron (red) of the S_4 state, plotted with isovalue: 0.02. A: In the X/Y plane, B: In the X/Z plane, C: In the Z/Y plane, D: 45° to the axes.

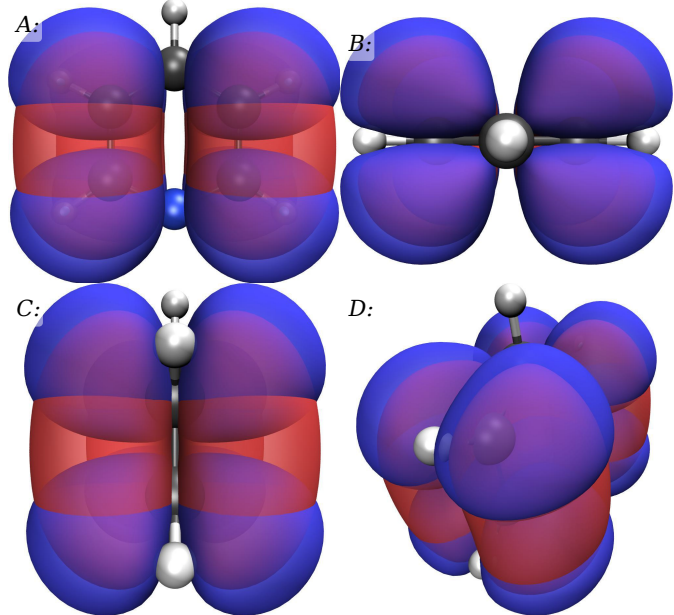


Figure 25: Density plot of the NTO hole (blue) & electron (red) of the S_6 state, plotted with isovalue: 0.02. A: In the X/Y plane, B: In the X/Z plane, C: In the Z/Y plane, D: 45° to the axes.

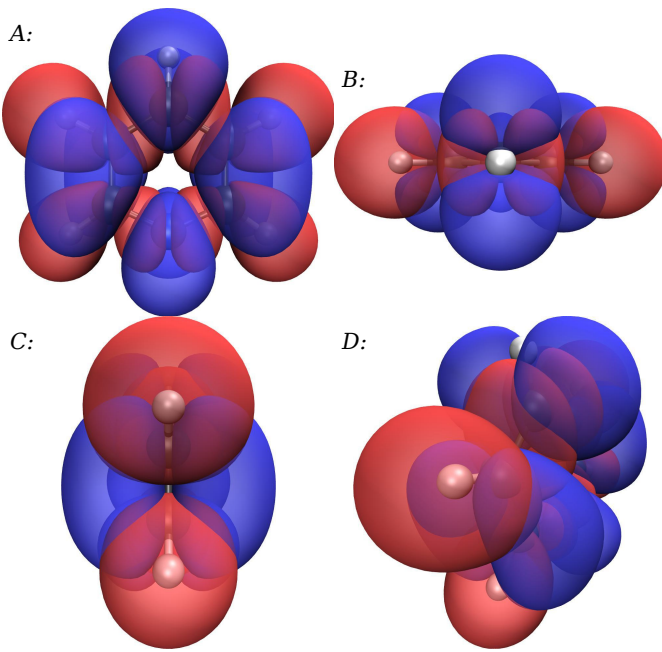


Figure 26: Density plot of the NTO hole (blue) & electron (red) of the S_7 state, plotted with isovalue: 0.02. A: In the X/Y plane, B: In the X/Z plane, C: In the Z/Y plane, D: 45° to the axes.

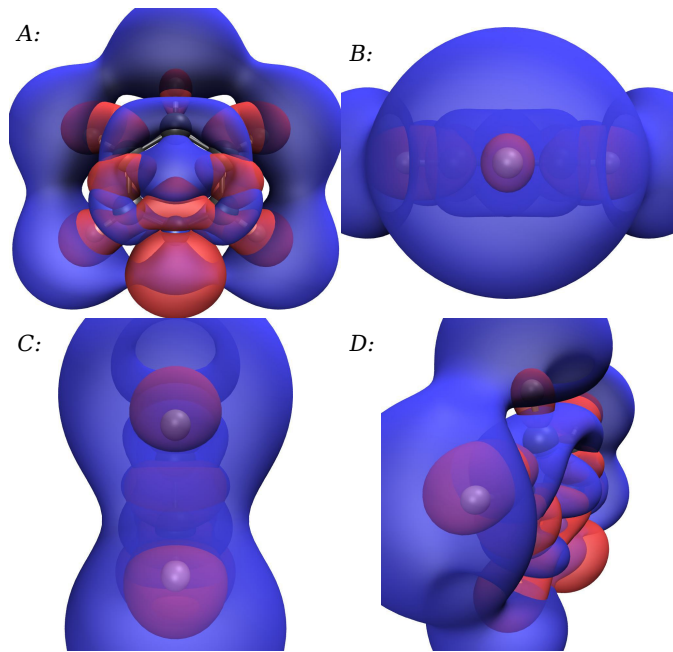


Figure 28: Density plot of the NTO hole (blue) & electron (red) of the S_9 state, plotted with isovalue: 0.02. A: In the X/Y plane, B: In the X/Z plane, C: In the Z/Y plane, D: 45° to the axes.

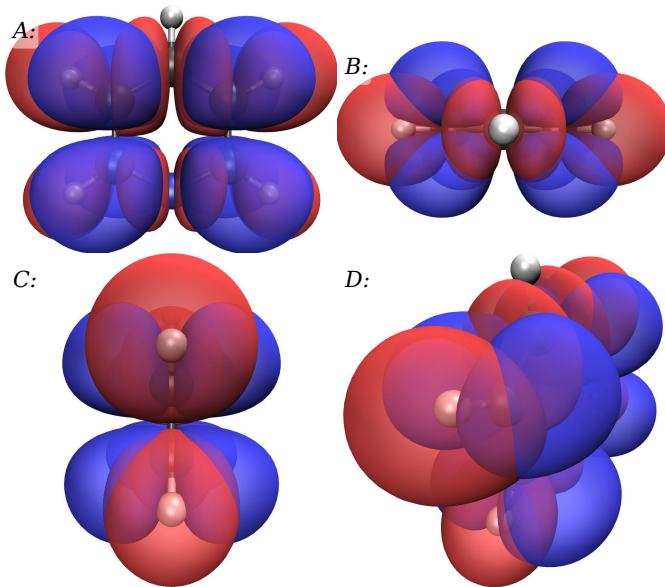


Figure 27: Density plot of the NTO hole (blue) & electron (red) of the S_8 state, plotted with isovalue: 0.02. A: In the X/Y plane, B: In the X/Z plane, C: In the Z/Y plane, D: 45° to the axes.

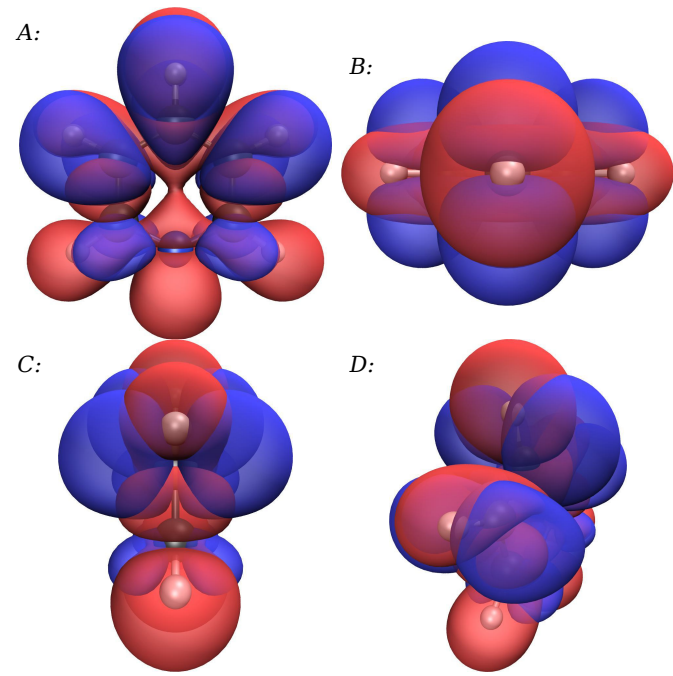


Figure 29: Density plot of the NTO hole (blue) & electron (red) of the S_{10} state, plotted with isovalue: 0.02. A: In the X/Y plane, B: In the X/Z plane, C: In the Z/Y plane, D: 45° to the axes.

Adiabatic Emission Energy

The adiabatic emission energy, corresponding to the difference in energy between an excited state at an excited state geometry, and the ground state at the ground state geometry, from the **S₁ state** to the ground state was calculated and found to be 4.62 eV. This energy is equivalent to emission of a photon with a wavelength of 268 nm, corresponding to a colour of Ultraviolet ■ and CIE coordinates (x,y) of (0.00, 0.00). The excited state had a total energy of -6743.99 eV and a multiplicity of one, while the ground state had a total energy of -6748.61 eV and a multiplicity of one. This emission is therefore a fluorescence type process, because both the ground and excited state have the same

multiplicity. Finally, the rate constant of the emission was calculated to be $5.01\text{e}+07 \text{ s}^{-1}$

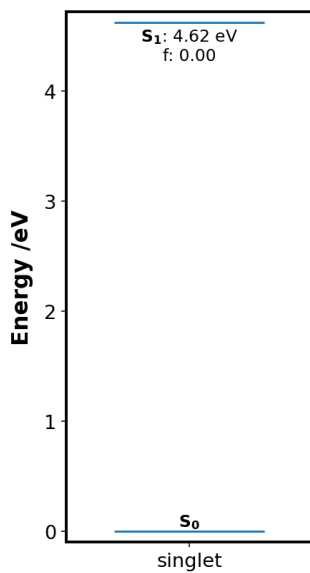


Figure 30: Graph of the calculated adiabatic S_1 emission energy.

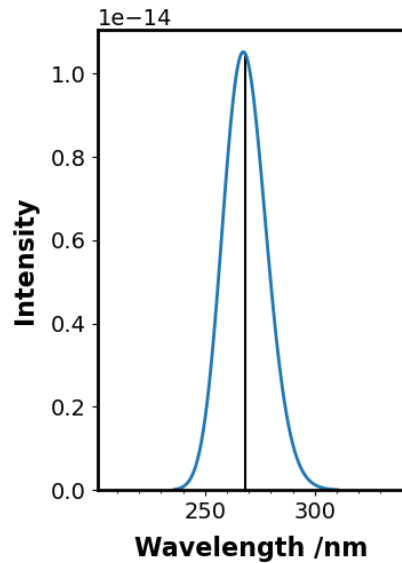


Figure 31: Graph of the simulated adiabatic S_1 emission spectrum. Excited states are shown as vertical black lines, while peaks simulated with a gaussian function with FWHM: 0.4 eV are shown as a blue line. Peaks can be found at: 267 nm.

Vertical Emission Energy

The vertical emission energy, corresponding to the difference in energy between an excited state at an excited state geometry, and the ground state at the ground state geometry, from the S_1 state to the ground state was calculated and found to be 4.12 eV. This energy is equivalent to emission of a photon with a

wavelength of 301 nm, corresponding to a colour of Ultraviolet ■ and CIE coordinates (x,y) of (0.00, 0.00). The excited state had a total energy of -6743.99 eV and a multiplicity of one, while the ground state had a total energy of -6748.11 eV and a multiplicity of one. This emission is therefore a fluorescence type process, because both the ground and excited state have the same multiplicity. Finally, the rate constant of the emission was calculated to be $3.54\text{e}+07 \text{ s}^{-1}$

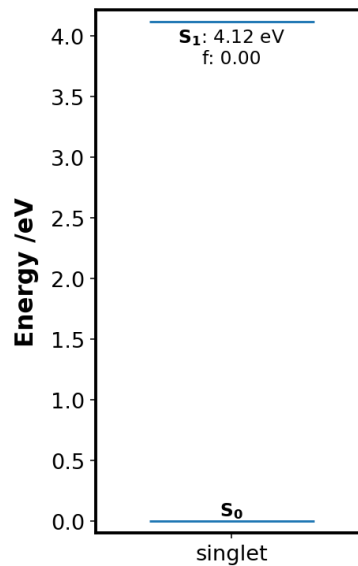


Figure 32: Graph of the calculated vertical S_1 emission energy.

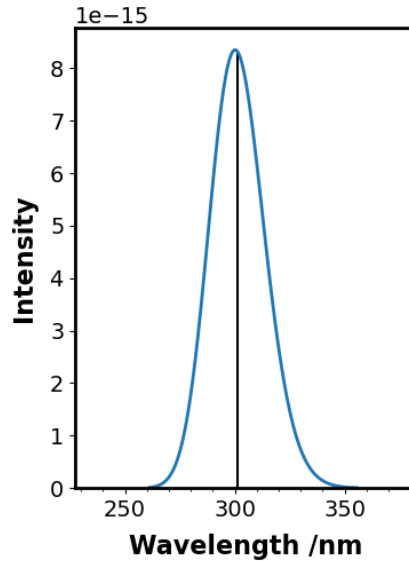


Figure 33: Graph of the simulated vertical S_1 emission spectrum. Excited states are shown as vertical black lines, while peaks simulated with a gaussian function with FWHM: 0.4 eV are shown as a blue line. Peaks can be found at: 300 nm.

Tables Of Results

Atom Coordinates

Table 12: Coordinates of the atoms of the system under study, as aligned to the cartesian axes by the Minimal method.

Element	X Coord /Å	Y Coord /Å	Z Coord /Å				
C	-1.1386600	-0.7199540	0.0000200	16	HOMO-5	A	-11.2778
C	-1.1953980	0.6709320	-0.0000220	15	HOMO-6	A	-11.9507
C	-0.0000260	1.3817850	-0.0000190	14	HOMO-7	A	-13.1140
C	1.1953740	0.6709710	-0.0000200	13	HOMO-8	A	-13.4217
C	1.1386890	-0.7199120	-0.0000270	12	HOMO-9	A	-14.7872
N	0.0000240	-1.4172140	0.0000620	11	HOMO-10	A	-17.5723
H	-2.0570650	-1.3046280	0.0000360	10	HOMO-11	A	-17.6352
H	-2.1540460	1.1794230	-0.0000390	9	HOMO-12	A	-21.3397
H	-0.0000390	2.4678210	-0.0000450	8	HOMO-13	A	-22.5449
H	2.1539990	1.1795060	-0.0000200	7	HOMO-14	A	-26.3953
H	2.0571100	-1.3045590	0.0000440	6	HOMO-15	A	-278.8609

Molecular Orbitals

Table 13: Energies of the calculated molecular orbitals.

Level	Label	Symmetry	Energy /eV				
37	LUMO+15	A	14.9940	6	A	768.8726	8.6373
36	LUMO+14	A	14.5273	7	A	904.9758	0.0000
35	LUMO+13	A	12.7428	8	A	966.8891	0.0014
34	LUMO+12	A	12.6081	9	A	1007.7254	0.0000
33	LUMO+11	A	9.0029	10	A	1019.4319	11.5446
32	LUMO+10	A	8.9866	11	A	1023.1818	0.0001
31	LUMO+9	A	8.3038	12	A	1061.1575	2.6424
30	LUMO+8	A	6.7868	13	A	1094.9181	0.0005
29	LUMO+7	A	5.2853	14	A	1106.3118	7.3922
28	LUMO+6	A	5.2515	15	A	1176.6064	2.3938
27	LUMO+5	A	4.6436	16	A	1254.2108	3.6314
26	LUMO+4	A	4.2561	17	A	1342.5154	0.0027
25	LUMO+3	A	4.2020	18	A	1388.6405	0.0269
24	LUMO+2	A	2.9309	19	A	1490.0899	36.1488
23	LUMO+1	A	-0.1420	20	A	1532.7236	4.9241
22	LUMO	A	-0.5097	21	A	1661.7273	12.3410
21	HOMO	A	-7.2829	22	A	1669.3960	32.4724
20	HOMO-1	A	-7.4475	23	A	3188.5029	38.3142
19	HOMO-2	A	-8.1539	24	A	3191.5774	11.3414
18	HOMO-3	A	-10.1324	25	A	3219.0592	5.9386
17	HOMO-4	A	-11.2402	26	A	3235.6160	22.7306
				27	A	3242.8238	5.1354

Vibrational Frequencies

Table 14: Energies of the calculated vibrational frequencies.

Number	Symmetry	Frequency /cm ⁻¹	Intensity /km mol ⁻¹
1	A	384.2445	0.0000
2	A	417.5700	4.1187
3	A	611.7278	5.2079
4	A	668.2642	0.4647
5	A	721.5500	61.5866
6	A	768.8726	8.6373
7	A	904.9758	0.0000
8	A	966.8891	0.0014
9	A	1007.7254	0.0000
10	A	1019.4319	11.5446
11	A	1023.1818	0.0001
12	A	1061.1575	2.6424
13	A	1094.9181	0.0005
14	A	1106.3118	7.3922
15	A	1176.6064	2.3938
16	A	1254.2108	3.6314
17	A	1342.5154	0.0027
18	A	1388.6405	0.0269
19	A	1490.0899	36.1488
20	A	1532.7236	4.9241
21	A	1661.7273	12.3410
22	A	1669.3960	32.4724
23	A	3188.5029	38.3142
24	A	3191.5774	11.3414
25	A	3219.0592	5.9386
26	A	3235.6160	22.7306
27	A	3242.8238	5.1354

Excited States

Table 11: Energies and other properties of the calculated excited states.

Number	Symbol	Symmetry	Energy /eV	Wavelength /nm	Colour (CIE x,y)	Oscillator Strength	Transitions (Probability)
1	T ₁	Triplet-A	4.2757	289.97	Ultraviolet [■] (0.00, 0.00)	0.0000	HOMO → LUMO (0.97) HOMO → LUMO+4 (0.02)
2	T ₂	Triplet-A	4.2914	288.91	Ultraviolet [■] (0.00, 0.00)	0.0000	HOMO-1 → LUMO+1 (0.67) HOMO-2 → LUMO (0.30) HOMO-4 → LUMO+4 (0.02)
3	T ₃	Triplet-A	4.6850	264.64	Ultraviolet [■] (0.00, 0.00)	0.0000	HOMO-1 → LUMO (0.97) HOMO-2 → LUMO+1 (0.03)
4	T ₄	Triplet-A	5.0511	245.46	Ultraviolet [■] (0.00, 0.00)	0.0000	HOMO-2 → LUMO (0.68) HOMO-1 → LUMO+1 (0.32)
5	S ₁	Singlet-A	5.0737	244.37	Ultraviolet [■] (0.00, 0.00)	0.0066	HOMO → LUMO (0.99)
6	T ₅	Triplet-A	5.2125	237.86	Ultraviolet [■] (0.00, 0.00)	0.0000	HOMO → LUMO+1 (1.00)
7	S ₂	Singlet-A	5.3747	230.68	Ultraviolet [■] (0.00, 0.00)	0.0000	HOMO → LUMO+1 (1.00)
8	S ₃	Singlet-A	5.7931	214.02	Ultraviolet [■] (0.00, 0.00)	0.0445	HOMO-1 → LUMO (0.69) HOMO-2 → LUMO+1 (0.30)
9	T ₆	Triplet-A	5.8469	212.05	Ultraviolet [■] (0.00, 0.00)	0.0000	HOMO-2 → LUMO+1 (0.96) HOMO-1 → LUMO (0.03)
10	S ₄	Singlet-A	6.8391	181.29	Ultraviolet [■] (0.00, 0.00)	0.0294	HOMO-1 → LUMO+1 (0.62) HOMO-2 → LUMO (0.35)
11	T ₇	Triplet-A	7.5290	164.68	Ultraviolet [■] (0.00, 0.00)	0.0000	HOMO-3 → LUMO (0.98)
12	T ₈	Triplet-A	7.8093	158.76	Ultraviolet [■] (0.00, 0.00)	0.0000	HOMO-4 → LUMO (0.83) HOMO-2 → LUMO+4 (0.16)
13	S ₅	Singlet-A	7.8387	158.17	Ultraviolet [■] (0.00, 0.00)	0.0000	HOMO-3 → LUMO (0.99)
14	T ₉	Triplet-A	7.8738	157.46	Ultraviolet [■] (0.00, 0.00)	0.0000	HOMO-3 → LUMO+1 (0.98)
15	S ₆	Singlet-A	7.9756	155.45	Ultraviolet [■] (0.00, 0.00)	0.8636	HOMO-2 → LUMO+1 (0.66) HOMO-1 → LUMO (0.27)
16	T ₁₀	Triplet-A	8.0844	153.36	Ultraviolet [■] (0.00, 0.00)	0.0000	HOMO-4 → LUMO+1 (0.65) HOMO-1 → LUMO+4 (0.34)
17	S ₇	Singlet-A	8.0937	153.19	Ultraviolet [■] (0.00, 0.00)	0.8783	HOMO-2 → LUMO (0.58) HOMO-1 → LUMO+1 (0.32) HOMO → LUMO+2 (0.02)
18	S ₈	Singlet-A	8.2671	149.97	Ultraviolet [■] (0.00, 0.00)	0.0069	HOMO-3 → LUMO+1 (0.99)
19	S ₉	Singlet-A	8.9279	138.87	Ultraviolet [■] (0.00, 0.00)	0.0000	HOMO-5 → LUMO (0.96) HOMO → LUMO+4 (0.03)
20	S ₁₀	Singlet-A	8.9578	138.41	Ultraviolet [■] (0.00, 0.00)	0.0000	HOMO-1 → LUMO+2 (0.99)

Transition Dipole Moments

Table 15: Properties of the calculated transition dipole moments. [a]: The electric transition dipole moment (TEDM), in Debye (D). [b]: Angle between the TEDM and the x-axis of the molecule. [c]: Angle between the TEDM and xy-plane of the molecule. [d]: The magnetic transition dipole moment (TMDM), in atomic units (au). [e]: Angle between the TMDM and the x-axis of the molecule. [f]: Angle between the TMDM and xy-plane of the molecule. [g]: The TEDM, in Gaussian CGS (centimetre, gram, second) units. [h]: The TMDM, in Gaussian CGS (centimetre, gram, second) units. [i]: The angle between the electric and magnetic transition dipole moments, in Gaussian CGS units. [j]: The cosine of the angle between the electric and magnetic transition dipole moments, in Gaussian CGS units. [k]: The dissymmetry factor of the transition dipole moment.

Excited State	$\mu^{[a]}$ Vector /D	$\mu^{[a]}$ /D	$\theta_{\mu,x}^{[b]}$ /°	$\theta_{\mu,xy}^{[c]}$ /°	$m^{[d]}$ Vector /au	$m^{[d]}$ /au	$\theta_{m,x}^{[e]}$ /°	$\theta_{m,xy}^{[f]}$ /°	$\mu^{[g]}$ /esu·cm	$m^{[h]}$ /erg·G ⁻¹	$\theta_{\mu,m}^{[i]}$ /°	$\cos(\theta_{\mu,m})^{[j]}$	$g_{lum}^{[k]}$
T ₁	0.00, 0.00, 0.00	0.00	0.00	0.00	0.00, 0.00, 0.00	0.00	0.00	0.00	0.00e+00	0.00e+00	90.00	0.00	0.000
T ₂	0.00, 0.00, 0.00	0.00	0.00	0.00	0.00, 0.00, 0.00	0.00	0.00	0.00	0.00e+00	0.00e+00	90.00	0.00	0.000
T ₃	0.00, 0.00, 0.00	0.00	0.00	0.00	0.00, 0.00, 0.00	0.00	0.00	0.00	0.00e+00	0.00e+00	90.00	0.00	0.000
T ₄	0.00, 0.00, 0.00	0.00	0.00	0.00	0.00, 0.00, 0.00	0.00	0.00	0.00	0.00e+00	0.00e+00	90.00	0.00	0.000
S ₁	0.00, -0.00, 0.59	0.59	90.00	89.98	0.69, 0.00, 0.00	0.69	0.00	0.00	5.88e-19	6.41e-21	90.00	0.00	0.000
T ₅	0.00, 0.00, 0.00	0.00	0.00	0.00	0.00, 0.00, 0.00	0.00	0.00	0.00	0.00e+00	0.00e+00	90.00	0.00	0.000
S ₂	0.00, 0.00, 0.00	0.00	0.00	0.00	-0.00, -0.03, 0.00	0.03	89.80	0.00	0.00e+00	2.68e-22	90.00	0.00	0.000
S ₃	-1.42, 0.00, 0.00	1.42	0.00	0.00	-0.00, 0.00, -0.18	0.18	89.97	89.97	1.42e-18	1.65e-21	90.03	-0.00	< 0.001
T ₆	0.00, 0.00, 0.00	0.00	0.00	0.00	0.00, 0.00, 0.00	0.00	0.00	0.00	0.00e+00	0.00e+00	90.00	0.00	0.000
S ₄	-0.00, -1.07, 0.00	1.07	89.99	0.00	0.00, 0.00, 0.00	0.00	0.00	0.00	1.07e-18	0.00e+00	90.00	0.00	0.000
T ₇	0.00, 0.00, 0.00	0.00	0.00	0.00	0.00, 0.00, 0.00	0.00	0.00	0.00	0.00e+00	0.00e+00	90.00	0.00	0.000

T ₈	0.00, 0.00, 0.00	0.00	0.00	0.00	0.00, 0.00, 0.00	0.00	0.00	0.00	0.00e+00	0.00e+00	90.00	0.00	0.000
S ₅	-0.00, -0.00, 0.00	< 0.01	33.69	0.00	0.00, -0.16, 0.00	0.16	90.00	0.00	9.16e-22	1.47e-21	123.69	-0.55	-0.995
T ₉	0.00, 0.00, 0.00	0.00	0.00	0.00	0.00, 0.00, 0.00	0.00	0.00	0.00	0.00e+00	0.00e+00	90.00	0.00	0.000
S ₆	5.34, -0.00, 0.00	5.34	0.01	0.00	0.00, 0.00, 0.04	0.04	90.00	90.00	5.34e-18	3.64e-22	90.00	0.00	0.000
T ₁₀	0.00, 0.00, 0.00	0.00	0.00	0.00	0.00, 0.00, 0.00	0.00	0.00	0.00	0.00e+00	0.00e+00	90.00	0.00	0.000
S ₇	-0.00, -5.35, -0.00	5.35	89.99	0.00	0.00, 0.00, 0.00	0.00	0.00	0.00	5.35e-18	0.00e+00	90.00	0.00	0.000
S ₈	-0.00, 0.00, -0.47	0.47	89.94	89.93	-0.33, 0.00, 0.00	0.33	0.00	0.00	4.68e-19	3.10e-21	90.06	-0.00	< 0.001
S ₉	0.00, -0.00, -0.00	< 0.01	90.00	86.42	1.25, -0.00, 0.00	1.25	0.00	0.00	4.07e-21	1.16e-20	90.00	-0.00	< 0.001
S ₁₀	0.00, -0.00, 0.00	< 0.01	90.00	0.00	0.00, 0.53, 0.00	0.53	89.99	0.00	2.54e-22	4.87e-21	0.01	1.00	0.208

References

1. N. M. O'boyle, A. L. Tenderholt and K. M. Langner, *Journal of Computational Chemistry*, 2008, **29**, 839-845
2. P. Virtanen, R. Gommers, T. E. Oliphant, M. Haberland, T. Reddy, D. Cournapeau, E. Burovski, P. Peterson, W. Weckesser, J. Bright, S. J. van der Walt, M. Brett, J. Wilson, K. Jarrod Millman, N. Mayorov, A. R. J. Nelson, E. Jones, R. Kern, E. Larson, C. Carey, I. Polat, Y. Feng, E. W. Moore, J. VanderPlas, D. Laxalde, J. Perktold, R. Cimrman, I. Henriksen, E. A. Quintero, C. R. Harris, A. M. Archibald, A. H. Ribeiro, F. Pedregosa, P. van Mulbregt and S. 1. 0. Contributors, *Nature Methods*, 2020, **17**, 261--272
3. T. Mansencal, M. Mauderer, M. Parsons, N. Shaw, K. Wheatley, S. Cooper, J. D. Vandenberg, L. Canavan, K. Crowson, O. Lev, K. Leinweber, S. Sharma, T. J. Sobotka, D. Moritz, M. Pppp, C. Rane, P. Eswaramoorthy, J. Mertic, B. Pearlstine, M. Leonhardt, O. Niemitalo, M. Szymanski and M. Schambach, Colour 0.3.15, Zenodo, 2020
4. K. Shizu and H. Kaji, *The Journal of Physical Chemistry A*, 2021, **125**, 9000--9010
5. W. Humphrey, A. Dalke and K. Schulten, *Journal of Molecular Graphics*, 1996, **14**, 33-38
6. J. Stone, Masters Thesis, Computer Science Department, University of Missouri-Rolla, 1998
7. J. D. Hunter, *Computing in Science & Engineering*, 2007, **9**, 90-95
8. M. Bayer, <https://www.makotemplates.org>, (accessed May 2020)
9. K. Community, <https://weasyprint.org>, (accessed May 2020)